



Faculty of Manufacturing Engineering

**DEVELOPMENT AND PERFORMANCE ANALYSIS OF ALUMINA-
YTTRIA STABILIZED ZIRCONIA-CHROMIA CUTTING TOOL
FOR HIGH WEAR PERFORMANCE**

Norfauzi bin Tamin

Doctor of Philosophy

2020

**DEVELOPMENT AND PERFORMANCE ANALYSIS OF ALUMINA-YTTRIA
STABILIZED ZIRCONIA-CHROMIA CUTTING TOOL FOR HIGH WEAR
PERFORMANCE**

NORFAUZI BIN TAMIN

**A thesis submitted
in fulfillment of the requirements for the degree of Doctor of Philosophy**

Faculty of Manufacturing Engineering

UNIVERSITI TEKNIKAL MALAYSIA MELAKA

2020

DECLARATION

I declare that this thesis entitled “Development and Performance Analysis of Alumina-Yttria Stabilized Zirconia-Chromia Cutting Tool for High Wear Performance” is the result of my own research except as cited in the references. The thesis has not been accepted for any degree and is not concurrently submitted in candidature of any other degree.


Signature : 

Name : NORFAUZI BIN TAMIN

Date : 3/12/2020

APPROVAL

I hereby declare that I have read this thesis and in my opinion this thesis is sufficient in terms of scope and quality for the award of Doctor of Philosophy.

Signature : 
PROF. MADYA IR. DR. MOHD HADZLEY BIN ABU BAKAR
Ketua Jabatan
Supervisor name : Jabatan Teknologi Industri
Fakulti Teknologi Kejuruteraan Mekanikal dan Pembuatan
Universiti Teknikal Malaysia Melaka
Date : 3/12/2020

DEDICATION

This project is dedicated to my beloved mother, father, wife and children for being great pillars of support.

ABSTRACT

Alumina based cutting tool have gradually garnered huge applications in refractory process especially in machining industries. This is due to their excellent hot hardness and abrasion resistance that could shear the workpiece material efficiently especially in dry condition. However, their inherent properties such as brittleness, low thermal shock resistance and sensitive to the cutting load have led to difficulty in providing longer tool life which limit their applications. This study presents the improvement of alumina (Al_2O_3) based cutting tool by addition of zirconia (ZrO_2) and chromia (Cr_2O_3) content. The development of these cutting tools were divided into four parts. The first part focused to determine the effective processing parameters with variations of polyethylene glycol (PEG) content (0.6-1.25 wt.%) as binder, sintering temperature (1200°C-1400°C) and cold isostatic pressing (CIP) pressure (200-400 MPa). The second part focused on the formulation of Al_2O_3 , ZrO_2 and Cr_2O_3 compositions to produce effective cutting tool based on the hardness, density, flexural strength and coefficient of friction (COF). Various content of ZrO_2 (0, 5, 10, 15, 20 and 25 wt.%) and Cr_2O_3 (0, 0.2, 0.4, 0.6 and 0.8 wt.%) were added into dominant Al_2O_3 powders and consistently processed by using parameters determined from the first part of study. The third part focused on the comparison of machining performance for the fabricated cutting tools based on the tool life and wear mechanism. The fourth part focused on the optimization of machining parameters based on the response surface methodology (RSM) and analysis of variance (ANOVA). The results from the first part highlighted that the effective content of PEG binder recorded at 0.6 wt%. The samples recorded maximum hardness and density at 62.5 HRc and 3.692 g/cm^3 when CIP pressure was set at 300 MPa and 60-second dwell time and the sintering temperature was set at 1400°C and 9 hours soaking time. For the second part of the study, Al_2O_3 - ZrO_2 with ratio 80-20 wt% produced hardness, relative density and bending strength of 70.07 HRc, 97% and 1449.33 MPa respectively. This value was changed to 71.03 HRc, 95.8% and 856.02 MPa when 0.6 wt% Cr_2O_3 were added into the 80-20 wt% Al_2O_3 - ZrO_2 . Al_2O_3 - ZrO_2 mixed Cr_2O_3 presented lower COF (0.23) as compared to Al_2O_3 - ZrO_2 (0.28) and Al_2O_3 (0.34). At the third part of the study, cutting tool fabricated from Al_2O_3 - ZrO_2 mixed Cr_2O_3 with ratio 80-20-0.6 wt.% recorded highest tool life of 360-second with 33.33% improvement of tool life as compared to 80-20 wt.% ZTA (240-second) and 75% improvement of pure Al_2O_3 (90-second). The optimization of cutting parameters on the final part of the study proposed that the cutting speed of 200 m/min, feed rate of 0.125 mm/rev and depth of cut 0.50 mm obtained 99% desirability to produce minimum wear rate. Overall, the addition of 0.6 wt.% Cr_2O_3 into Al_2O_3 - ZrO_2 matrix adequately enough to evaporate and reacted with the Al_2O_3 to generate anisotropy-oriented particles at the upper surface of the product. Such structure enabled stronger particle compact formed due to the interlocking grains at the affected area.

ABSTRAK

Alat pemotong berasaskan alumina secara beransur-ansur menghasilkan aplikasi yang sangat besar dalam proses refraktori terutamanya dalam industri pemesinan. Ini disebabkan kekerasan panas dan ketahanan lelasan yang sangat baik yang boleh memotong bahan kerja dengan cekap terutama dalam keadaan kering. Walau bagaimanapun, sifat-sifat yang wujud seperti kerapuhan, rintangan kejutan haba yang rendah dan sensitif terhadap beban pemotongan telah menyebabkan kesukaran dalam menyediakan hayat alat yang lebih lama yang membataskan aplikasi mereka. Kajian ini membentangkan fabrikasi dan prestasi pemesinan alat pemotong yang dibuat berasaskan alumina (Al_2O_3) dengan penambahan zirkonia (ZrO_2) dan chromia (Cr_2O_3). Pembangunan alat pemotong ini dibahagikan kepada empat bahagian. Bahagian pertama memberi tumpuan kepada penentuan parameter pemprosesan yang berkesan dengan variasi kandungan polyethylene glycol (PEG) (0.6-1.25% berat) sebagai pengikat, suhu persinteran ($1200^{\circ}C$ - $1400^{\circ}C$) dan tekanan isostatik sejuk (CIP) (200-400 MPa). Bahagian kedua memberi tumpuan kepada penggubalan komposisi Al_2O_3 , ZrO_2 dan Cr_2O_3 untuk menghasilkan alat pemotong yang berkesan berdasarkan kekerasan, kepadatan, kekuatan lenturan dan pekali geseran (COF). Bahagian ketiga memberi tumpuan kepada perbandingan prestasi pemesinan terhadap alat pemotong yang difabrikasi berdasarkan hayat alat dan mekanisma haus. Bahagian keempat memberi tumpuan kepada pengoptimuman parameter pemesinan berdasarkan kaedah tindak balas permukaan (RSM) dan variasi analisis (ANOVA). Keputusan daripada bahagian pertama menekankan bahawa kandungan pengikat PEG yang berkesan direkodkan pada 0.6% berat. Sampel telah mencatatkan kekerasan dan ketumpatan maksimum pada 62.5 HRc dan 3.692 g/cm^3 apabila tekanan CIP ditetapkan pada 300 MPa serta 60 saat masa tinggal dan suhu persinteran pula ditetapkan pada $1400^{\circ}C$ dan 9 jam waktu perendaman. Pada bahagian kedua kajian, Al_2O_3 - ZrO_2 dengan nisbah 80-20% berat menghasilkan kekerasan, ketumpatan relatif dan kekuatan lentur 70.07 HRc, 97% dan 1449.33 MPa masing-masing. Nilai ini telah berubah kepada 71.03 HRc, 95.8% dan 856.02 MPa apabila 0.6% berat Cr_2O_3 ditambah ke dalam 80-20% berat ZTA. ZTA dicampur Cr_2O_3 memperoleh nilai COF yang lebih rendah (0.23) berbanding ZTA (0.28) dan Al_2O_3 (0.34). Pada bahagian ketiga kajian, alat pemotong yang dibuat dari ZTA dicampur Cr_2O_3 dengan nisbah 80-20-0.6% berat mencatatkan hayat alat tertinggi iaitu 360 saat dengan peningkatan 33.33% berbanding 80-20% berat ZTA (240 saat) dan peningkatan 75% daripada Al_2O_3 tulen (90 saat). Pengoptimuman parameter pemotongan pada bahagian akhir kajian mencadangkan bahawa kelajuan pemotongan 200 m/min, kadar suapan 0.125 mm/rev dan kedalaman pemotongan 0.50 mm memperoleh 99% keinginan. Secara keseluruhannya, penambahan 0.6% berat Cr_2O_3 kepada matriks Al_2O_3 - ZrO_2 sangat mencukupi untuk Cr_2O_3 menguap dan bertindak balas dengan struktur matrik Al_2O_3 bagi menghasilkan zarah berorientasikan anisotropi di permukaan atas produk. Struktur ini membolehkan zarah padat kuat terbentuk disebabkan oleh biji-bijian saling terkunci antara satu sama lain di kawasan yang terjejas.

ACKNOWLEDGEMENTS

First and foremost, I would like to express my greatest gratitude to Almighty God, Allah S.W.T for giving me strength and courage to completed my study with the best I could. Indeed, without His Help and Well, nothing will be accomplished.

I would like to take this opportunity to express my sincere acknowledgement to my supervisor Associate Professor Ir. Dr. Mohd Hadzley bin Abu Bakar from the Faculty of Manufacturing Engineering for his essential supervision, support and encouragement towards the completion of this thesis. I would also like to express my greatest gratitude to Associate Professor Ts. Dr. Umar Al-Amani bin Azlan from Faculty of Mechanical and Manufacturing Engineering Technology, co-supervisor of this project for his advice and encouragement for this research.

Most importantly, my sincere appreciation goes to my beloved wife, Norazreen binti Tumiran for his love, patience and endless support throughout this journey. Special thanks to my beloved mother and father, Fatimah binti Rais and Tamin bin Kastawi and siblings for their moral support in completing this degree. To my children, Muhammad Haiqal Danish, Nuraleesya Damia, Muhammad Hafiy Darwish and Nurarissa Diana, thank you for being patient with your father. Lastly, thank you to everyone who had been to the crucial parts of realization of this project.

TABLE OF CONTENTS

	PAGE
DECLARATION	
APPROVAL	
DEDICATION	
ABSTRACT	i
ABSTRAK	ii
ACKNOWLEDGEMENTS	iii
TABLE OF CONTENTS	iv
LIST OF TABLES	vii
LIST OF FIGURES	ix
LIST OF APPENDICES	xix
LIST OF ABBREVIATIONS	xx
LIST OF SYMBOLS	xxii
LIST OF PUBLICATIONS	xxiii
CHAPTER	
1. INTRODUCTION	1
1.1 Background of study	1
1.2 Problem statement	4
1.3 Objective	5
1.4 Project scope	6
2. LITERATURE REVIEW	9
2.1 Introduction	9
2.2 Physical of ceramic cutting tool	10
2.2.1 Properties of ceramics	12
2.2.2 Fracture toughness of ceramics	14
2.2.3 Ceramic hardness	15
2.2.4 Ceramic stress and its development	17
2.3 Alumina-based ceramic cutting tool	19
2.3.1 Alumina (Al_2O_3)	23
2.3.2 Zirconia (ZrO_2)	24
2.3.3 Chromium (III) oxide (Cr_2O_3)	28
2.4 ZrO_2 and Al_2O_3 effects on structures	31
2.5 Solid-state process grinding and mixing	32
2.5.1 Agglomerate	33
2.6 Cold isostatic press (CIP)	34
2.6.1 Type of CIP	35
2.7 Sintering	36
2.7.1 Sintering effect	38
2.8 Cutting tool design	39
2.9 Turning process	41
2.10 Tool wear	42

2.11	Tool life	46
2.12	Machinability of carbon steel	49
	2.12.1 Carbon steel	49
	2.12.2 Medium carbon steel (AISI 1045)	51
2.13	Previous research	52
2.14	Summary	66
3.	METHODOLOGY	67
3.1	Introduction	67
	3.1.1 Mould development	69
	3.1.2 Powder mixing	71
	3.1.3 Sieving and pressing	73
	3.1.4 Cold isostatic pressing (CIP)	74
	3.1.5 Sintering	76
3.2	Properties analysis for the fabricated ceramic cutting tool	77
	3.2.1 Density	79
	3.2.2 Hardness	81
	3.2.3 Flexural strength	81
	3.2.4 Analysis of failure modes and wear mechanisms	83
	3.2.5 Microstructure, crystal structure and wear mechanism analysis	85
	3.2.5.1 Sample preparation for SEM	85
	3.2.5.2 X-ray diffraction (XRD) machine	88
3.3	Machining evaluation	88
3.4	Design of Experiment	92
3.5	Summary	94
4.	RESULT AND DISCUSSION	95
4.1	Effect of binder addition into shape of ceramic mixture (Objective 1)	95
	4.1.1 Effect of PEG addition on density and hardness	97
	4.1.2 Effect of cold isotactic press (CIP) pressure on density and hardness	101
	4.1.2.1 Hardness effect on CIP	103
	4.1.3 Effect of sintering temperature on density and hardness	104
	4.1.3.1 Effect of ZrO ₂ on density and hardness	108
	4.1.4 Effect of Cr ₂ O ₃ content on density, hardness and flexural strength for Al ₂ O ₃ -ZrO ₂	110
4.2	Comparison of density, hardness and flexural strength of ZTA and ZTA mixed Cr ₂ O ₃ (Objective 2)	113
	4.2.1 Comparison of density of Al ₂ O ₃ -ZrO ₂ and Al ₂ O ₃ -ZrO ₂ -Cr ₂ O ₃	114
	4.2.2 Comparison of hardness of Al ₂ O ₃ -ZrO ₂ and Al ₂ O ₃ -ZrO ₂ -Cr ₂ O ₃	115
	4.2.3 Effect of ZrO ₂ and Cr ₂ O ₃ on flexural strength	117
	4.2.4 Microstructure analysis for Al ₂ O ₃ , ZTA and ZTA mixed Cr ₂ O ₃	120

4.3	Machining performance (Objective 3)	132
4.3.1	Al ₂ O ₃ cutting tool	132
4.3.2	ZTA cutting tool	134
4.3.3	ZTA mixed Cr ₂ O ₃ cutting tool	137
4.3.4	Comparison of performance between Al ₂ O ₃ , ZTA and ZTA mixed Cr ₂ O ₃	141
4.3.5	Wear formation and characteristics of Al ₂ O ₃ cutting tool	145
4.3.5.1	ZTA cutting tool	148
4.3.5.2	ZTA mixed Cr ₂ O ₃	150
4.3.6	Wear mechanism of Al ₂ O ₃ , ZTA and ZTA mixed Cr ₂ O ₃	154
4.3.6.1	Chipping that consequently inducing cracks or breakage	154
4.3.6.2	Particles loss that created abrasive actions	156
4.3.6.3	Molten metal attachment that forms built-up edge (BUE) and adhesive wear	159
4.4	Statistical modelling (Objective 4)	163
4.4.1	RSM and their results for machining ZTA mixed Cr ₂ O ₃	163
4.4.2	Analysis of process parameters of flank wear on ZTA mixed Cr ₂ O ₃	164
4.4.3	Diagnostic of the tool wear case study	167
4.4.4	Determination of significant factors influencing tool wear	169
4.4.5	Optimization of machining parameters based on the cutting speed, feed rate and depth of cut	172
4.4.6	Model validation	175
4.5	Summary	176
5.	CONCLUSION AND RECOMMENDATIONS	177
5.1	Conclusions	177
5.1.1	Processing aspect (Objective 1)	177
5.1.2	Mechanical behaviour and properties (Objective 2)	178
5.1.3	Machining aspect (Objective 3 and 4)	179
5.2	Recommendations for future work	180
	REFERENCES	182
	APPENDICES	208

LIST OF TABLES

TABLE	TITLE	PAGE
2.1	Properties of various ceramics at room temperature (Smuk et al., 2003)	12
2.2	Properties of various percentages of ceramics at room temperature (Sarkar et al., 2007)	14
2.3	Details of alumina purity properties (Choi et al., 2003)	21
2.4	General properties of Al ₂ O ₃ ceramic powder with percentages of mix (Choi et al., 2003)	21
2.5	Details about zirconia powder (Choi et al., 2003)	27
2.6	General properties of ZrO ₂ ceramic powder at certain percentages (Rittidech et al., 2013)	27
2.7	Range of n value	48
2.8	Mechanical properties of AISI 1045 (Ibrahim et al., 2015)	51
2.9	Chemical composition of AISI 1045 (Ibrahim et al., 2015)	52
2.10	Turning process parameter (Cheng et al., 2016)	58
2.11	Turning process parameter (Tan et al., 2018)	60
2.12	Mechanical behaviour and properties of ceramic cutting tool	61
2.13	Machining performance on ceramic cutting tool	63
3.1	The composition of (a) Al ₂ O ₃ and ZrO ₂ and (b) Cr ₂ O ₃	72

3.2	Unit conversion for CIP pressure	75
3.3	Process parameters with number of levels	75
3.4	Sintering temperature on study of binder, peg and temperature effect	76
3.5	Value of cutting speed and feed rate that used in this experiment for each of Al_2O_3 , $\text{Al}_2\text{O}_3\text{-ZrO}_2$ and $\text{Al}_2\text{O}_3\text{-ZrO}_2\text{-Cr}_2\text{O}_3$ fabricated cutting tool	91
4.1	The effect of various PEG percentages on ceramic density and porosity	98
4.2	Density and porosity result	108
4.3	HRc of various percentages	108
4.4	Density of variety Cr_2O_3 wt. %	110
4.5	The results of relative density, hardness and flexural strength obtained	114
4.6	Design of experiments and results for machining ZTA mixed Cr_2O_3	164
4.7	Fit summary for Cutting tool model	164
4.8	ANOVA on flank wear for cutting tool ZTA mixed with Cr_2O_3 before eliminating the insignificant terms	165
4.9	New ANOVA on the flank wear of cutting tool after eliminated the insignificant terms	166
4.10	Goals for factors and responses in finding the optimum parameters of cutting tool ZTA mixed Cr_2O_3	172
4.11	Optimisation parameters suggested by RSM for minimum tool wear	173
4.12	Optimisation parameters suggested by RSM for maximum tool wear	174
4.13	Confirmation results	175

LIST OF FIGURES

FIGURE	TITLE	PAGE
1.1	Comparison of important properties of ceramic and carbide cutting tools	7
1.2	Schematic diagram for scope of research	8
2.1	Ceramic cutting tool (Singh et al., 2016)	9
2.2	Effect of density on hardness of Al ₂ O ₃ (Wang and Hon, 1999)	16
2.3	Effect of temperature on hardness of Al ₂ O ₃ (Wang and Hon, 1999)	16
2.4	Temperature distribution on surface of cutting tool (a) short term and (b) long term (Zhao, 2014)	18
2.5	Distribution of temperature and thermal stress on ceramic cutting tools (Zhang et al., 2009)	19
2.6	O ²⁻ ions compilation around Al ³⁺ ions in Al ₂ O ₃ (Callister and Rethwisch, 2007)	20
2.7	Crystal structure of Al ₂ O ₃ mineral corundum (Soo and Min, 2011)	23
2.8	Preparation of O ions in the vicinity of Zr ions in ZrO ₂ (Han and Zhu, 2013)	25
2.9	Crystal structure of ZrO ₂ (a) cubic, (b) tetragonal, and (c) monoclinic (Callister and Rethwisch 2011)	26

2.10	Crystal structure of Cr ₂ O ₃ mineral corundum (Doh et al., 2000)	28
2.11	Sintered density (percentage of theoretical density) as a function of Cr ₂ O ₃ (Manshor et al., 2016)	29
2.12	Fracture toughness of Al ₂ O ₃ based cutting tool with different wt.% of Cr ₂ O ₃ (Manshor et al., 2016)	30
2.13	SEM micrographs of crack induced on surface of ZTA-TiO ₂ composite with addition of (a) 0 wt.% Cr ₂ O ₃ and (b) 0.6 wt.% Cr ₂ O ₃ (Manshor et al., 2016)	31
2.14	Schematic of ball and jars (Burmeister and Kwade, 2013)	33
2.15	Schematic of (a) dry bag and (b) wet bag CIP (Ćurković et al., 2015)	35
2.16	Pore morphology and network structure of sintered porous ceramics (a) 1150°C, (b) 1175°C, (c) 1200°C, (d) 1225°C, (e) 1250°C and (f) typical connection of grains (Liu et al., 2014)	37
2.17	Effect of temperature on the density of Sintered body (Santos et al., 2008)	38
2.18	The relative density and grain size of ceramics with different sintering times (Santos et al., 2008)	39
2.19	The effect of the strength of the cutting tool (Senthilkumar and Tamizharasan, 2014)	40
2.20	Geometry of single point cutting tool (Girsang and Dhupia, 2015)	40
2.21	Illustration of wear area of cutting tool during lathe machining (Smith, 2008)	43
2.22	Catastrophic failure of cutting tool (Abu Bakar et al., 2018)	45
2.23	Tool wear zone (Senthilkumar and Tamizharasan, 2014)	46

2.24	Wear on turning cutting tool following ISO 3685 standard (Luka et al., 2015)	47
2.25	Shows a typical measurement of flank wear and crater in accordance with the standard ISO: 3685	48
3.1	Flowchart of pilot study for first stage of ceramic cutting tool development	68
3.2	Drawing of (a) rhombus and (b) round shape by using CATIA V5 R23 software	70
3.3	3 Moulds assembly of (a) rhombus and (b) round	71
3.4	Ceramics powder (a) Al ₂ O ₃ (creamy colour), (b) ZrO ₂ (white colour), (c) Cr ₂ O ₃ (green colour) and (d) Polyethylene glycol (PEG) (liquid)	71
3.5	Preparation to mix the ceramic powder (a) weighing scale (b) plastic bottle and (c) ceramics ball	72
3.6	Specification of (a) ball mill machine and (b) ball mill parameter setting	73
3.7	Process to form a green body	74
3.8	Hard steel mesh basket put on to CIP machine model AIP3-12-60C	75
3.9	Sintering profile of 1400°C	76
3.10	Furnace brand Nabertherm model LH15/12	77
3.11	Analysis of ceramic cutting tool and machining capability test	78
3.12	Electronic densimeter brand Mitutoyo model MD-300S	80
3.13	Electronic densimeter (a) weighing sample and (b) soaked sample	80
3.14	Rockwell hardness machine brand Mitutoyo model HR-430MS	81

3.15	Universal testing machine (UTM) brand Instron model 5969	82
3.16	Three-point bending test (Ćurković et al., 2010)	83
3.17	Tool maker microscope brand Mitutoyo model MM-800	84
3.18	Tool wear measurement on the Mitutoyo Toolmaker microscope	84
3.19	Scanning electron microscopy (SEM) machine brand Zeiss model EVO 50	85
3.20	Polishing machine for grinding and polishing method	86
3.21	Ultrasonic bath machine	86
3.22	Ceramic cutting tool on the furnace machine	86
3.23	Thermal etching graph	87
3.24	Coating machine	87
3.25	X-ray diffraction (XRD) brand D8 Advance model MSE 4003	88
3.26	Three cutting tool type that needs to be compared (a) Al ₂ O ₃ (White), (b) Al ₂ O ₃ + ZrO ₂ (Creamy) and (c) Al ₂ O ₃ + ZrO ₂ mixed Cr ₂ O ₃ (Purple)	89
3.27	Ceramic cutting tool	89
3.28	Tool holder	89
3.29	Cutting material carbon steel AISI 1045	90
3.30	CNC Lathe machine brand HAAS model SL 20	90
3.31	CNC program for experiment	91
3.32	CNC turning operation for cleaning the workpiece surface before the experiment	92
3.33	RSM approach flow chart	93
4.1	Green body of the cutting tool without PEG	96

4.2	Green body and physical condition after sintering of ceramic cutting tool with binding agent	97
4.3	Density of PEG percentage	98
4.4	Effect of PEG on HRc	99
4.5	Comparison of microstructure focusing at Mag 1000 with 10 μm on ceramic cross sections of various PEG at (a) 0.6 wt.%, (b) 0.75 wt.%, (c) 1.0 wt.% and (d) 1.25 wt.%	100
4.6	Microstructure from top surface focusing at Mag 2000 with 2 μm (a) 0.6 wt.%, (b) 0.75 wt.%, (c) 1.0 wt.% and (d) 1.25 wt.%	101
4.7	The effect of CIP pressure on relative density of ceramics mixing	102
4.8	Effect of HRc on CIP pressure	104
4.9	The effect of sintering temperature on relative density for 90 wt.% Al_2O_3 -10 wt.% ZrO_2 sample	105
4.10	Microstructure from top surface focusing at Mag 2000 with 2 μm image of 90 wt.% Al_2O_3 -10 wt.% ZrO_2 sample at (a) 1400°C and (b) 1300°C	106
4.11	Effect sintering temperature on hardness for 90 wt.% Al_2O_3 -10 wt.% ZrO_2 sample	107
4.12	Effect of ZrO_2 content on (a) relative density and (b) hardness	109
4.13	Effect of Cr_2O_3 content on the density	111
4.14	Effect of Cr_2O_3 content on the hardness	112
4.15	Effect of Cr_2O_3 content on the flexural strength	112
4.16	Relative density of various samples in Al_2O_3 - ZrO_2	115
4.17	HRc on Composition of ZTA and ZTA mixed Cr_2O_3	116

4.18	Comparison between Al ₂ O ₃ -ZrO ₂ and Al ₂ O ₃ -ZrO ₂ mixed Cr ₂ O ₃	118
4.19	Mechanism of ZrO ₂ coalescence	119
4.20	Illustration of slip particles on grain boundaries (Jiang et al., 2014)	120
4.21	Cutting tool comparison between (a) Al ₂ O ₃ -ZrO ₂ and (b) Al ₂ O ₃ -ZrO ₂ - Cr ₂ O ₃	121
4.22	XRD patterns of 80 wt.% Al ₂ O ₃ -20 wt.% ZrO ₂ mixed 0.6 wt.% Cr ₂ O ₃	121
4.23	XRD pattern of different wt.% ZrO ₂ in ZTA	122
4.24	XRD identification of Al ₂ O ₃	123
4.25	XRD identification of ZrO ₂	124
4.26	Crystal structure of ZrO ₂ (a) cubic, (b) tetragonal, and (c) monoclinic. Red and blue spheres correspond to oxygen and zirconium atoms, respectively (Callister and Rethwisch, 2011)	125
4.27	Microstructure comparison of top surface views focusing at Mag 5000 with 1 μm	128
4.28	Surface comparison focusing at Mag 5000 with 1 μm image between (a) 100 wt.% Al ₂ O ₃ , (b) 80 wt.% Al ₂ O ₃ - 20 wt.% ZrO ₂ and (c) 80 wt.% Al ₂ O ₃ - 20 wt.% ZrO ₂ - 0.6 wt.% Cr ₂ O ₃	129
4.29	Surface comparison between (a) 95 wt.% Al ₂ O ₃ - 5wt.% ZrO ₂ and (a) 85 wt.% Al ₂ O ₃ - 15 wt.% ZrO ₂	130
4.30	Surface comparison between (a) 80 wt.% Al ₂ O ₃ - 20 wt.% ZrO ₂ and (b) 80 wt.% Al ₂ O ₃ - 20 wt.% ZrO ₂ - 0.6 wt.% Cr ₂ O ₃	131
4.31	Values of flank wear at different cutting speeds at feed rate of 0.10 mm/rev	132

4.32	Values of flank wear at different cutting speeds at feed rate 0.125 mm/rev	133
4.33	Values of flank wear at different cutting speeds at feed rate 0.150 mm/rev	133
4.34	Values of flank wear at different cutting speeds at feed rate 0.175 mm/rev	134
4.35	Values of flank wear at different cutting speeds of feed rate at 0.100 mm/rev	135
4.36	Values of flank wear at different cutting speeds at feed rate of 0.125 mm/rev	135
4.37	Values of flank wear at different cutting speeds at feed rate of 0.150 mm/rev	136
4.38	Values of flank wear at different cutting speeds at feed rate of 0.175 mm/rev	137
4.39	Values of flank wear at different cutting speeds at feed rate of 0.10 mm/rev	138
4.40	Values of flank wear at different cutting speeds at feed rate of 0.125 mm/rev	139
4.41	Values of flank wear at different cutting speeds at feed rate of 0.150 mm/rev	140
4.42	Values of flank wear at different cutting speeds at feed rate of 0.175 mm/rev	141
4.43	Comparison of tool life of cutting tools at cutting speed of 200 m/min	142
4.44	Comparison of tool life of cutting tool at cutting speed of 250 m/min	142

4.45	Comparison of tool life of cutting tools at feed rate of (a) 0.125 mm/rev and (b) 0.175 mm/rev	144
4.46	The cutting tool movement at the beginning of the touch of the AISI 1045 depending on the feed rate	145
4.47	Wear rate of 0.11mm at 32s	145
4.48	wear rate of 0.17mm at 63s	146
4.49	Wear rate of 0.22 mm at 94s	146
4.50	wear rate of 0.30 mm at 113s	146
4.51	Wear development of Al ₂ O ₃ cutting tool at machining time (a) 19s and wear rate 0.16mm and (b) 20s and wear rate 0.30mm	147
4.52	Wear development of ZTA at cutting speed of 200 m/min and feed rate of 0.125 mm/rev	148
4.53	Wear development of ZTA at cutting speed of 300 m/min and feed rate of 0.125 mm/rev	149
4.54	Wear development of ZTA mixed Cr ₂ O ₃ at cutting speed of 200 m/min and feed rate of 0.125 mm/rev	151
4.55	Wear characteristic at feed rate of 0.150 mm/rev	152
4.56	Wear mechanism of (a) Al ₂ O ₃ , (b) ZTA dan (c) ZTA mixed Cr ₂ O ₃ at 60 sec recorded at cutting speed of 200 m/min and feed rate of 0.125 mm/rev	153
4.57	Effect of cutting speed of 300 m/min and feed rate of 0.125 mm/rev on cutting tool of (a) Al ₂ O ₃ , (b) ZTA and (c) ZTA mixed Cr ₂ O ₃	154
4.58	Chipping shapes on cutting point that occur at 300 m/min cutting speed and feed rate of 0.100 mm/rev against Al ₂ O ₃ cutting tool	155

4.59	ZTA cutting tool showing horizontal propagation crack on flank face with cutting speed of 250 mm/min, feed rate of 0.175 mm/rev and depth of cut of 0.75 mm	156
4.60	Illustration of the formation of a parallel and groove boundary due to particle slippage along the wear area	157
4.61	Ceramic cutting tools that can be seen in the mixtures on ZTA mixed Cr ₂ O ₃ cutting tool with cutting speed of 300 m/min and feed rate of 0.125 mm/rev	157
4.62	Groove and parallel boundaries formed on ZTA mixed Cr ₂ O ₃ cutting tool that have been machined at cutting speed of 350 mm/min and feed rate of 0.125 mm/rev	158
4.63	Illustration of a single broken grain that is dragged out and gives shear force to grain around it to come out together	159
4.64	The fragments attached to the edge of the Al ₂ O ₃ cutting tool at cutting speed 200 m/min and federation 100 mm/rev	160
4.65	ZTA cutting tool that shows ceramic particles are broken into crater wear at 350 mm/min cutting speed and feed rate of 0.150 mm/rev	160
4.66	Debris attached to the edge of the cutting tool on the ZTA mixed Cr ₂ O ₃ cutting speed of 350 m/min and feed rate of 0.100 mm/rev	162
4.67	Chips that are stuck between cutting tools and AISI 1045	163
4.68	Normal probability plot for residuals data	168
4.69	Experiment residual versus predicted plot	168
4.70	Box Cox plot for transformation	169

4.71	Response surface on the tool wear of ZTA mixed Cr ₂ O ₃ between cutting speed and feed rate	170
4.72	Response surface on the tool wear of ZTA mixed Cr ₂ O ₃ between feed rate and depth of cut	171

LIST OF APPENDICES

APPENDIX	TITLE	PAGE
A	Flank wear of Al ₂ O ₃ cutting tool via toolmaker microscope	208
B	Flank wear of ZTA cutting tool via tool maker microscope	212
C	Flank wear of ZTA mixed Cr ₂ O ₃ cutting tool via tool maker microscope	218

LIST OF ABBREVIATIONS

AISI	-	American iron and steel institute
Al	-	Aluminium
Al ₂ O ₃	-	Aluminium oxide/ alumina
ASTM	-	American Society for Testing and Materials
BUE	-	Built-up edge
CBN	-	Cubic boron nitride
CeO ₂	-	Cerium oxide
CIP	-	Cold isotactic press
CNC	-	Computer numerical control
CrN	-	Chromium nitride
Cr ₂ O ₃	-	Chromium oxide
DOC	-	Depth of cut
EN	-	Euro norm
F _f	-	Load at fracture
F _r	-	Feed rate
HIP	-	Hot isotactic press
HSS	-	High speed steel
ISO	-	International standard organization
L	-	Distance